Title: A framework to improve predictions of warming effects on consumer-resource interactions

Running head: Temperature-dependence of consumer-resource interactions

Keywords: climate change, consumer-resource dynamics, food webs, community stability, biomass distributions, interaction strength, temperature dependence.

Authors: Alexis D. Synodinos[1*], Bart Haegeman[1], Arnaud Sentis[2], José M. Montoya[1]

[1]Station d'Ecologie Théorique et Expérimentale, CNRS, Moulis, 09200, France

[2]INRAE, Aix Marseille Univ., UMR RECOVER, 3275 route Cézanne, 13182 Aix-en-Provence, France.

***** Correspondence to

Alexios Synodinos, Station d'Ecologie Théorique et Expérimentale, UMR 5321, Moulis, 09200, France, Tel : +33 561 04 05 89, email : alexios.synodinos@sete.cnrs.fr

Author emails:

Bart Haegeman: bart.haegeman@sete.cnrs.fr

Arnaud Sentis: arnaud.sentis@inrae.fr

José M. Montoya: josemaria.montoyateran@sete.cnrs.fr

Author contributions: ADS, BH, AS and JMM conceived the framework. ADS and BH developed the method, AS and JMM guided its application. ADS led the writing of the

manuscript; BH, AS and JMM provided crucial input and guidance throughout the writing process. JMM obtained the funding and managed the project. The authors declare no competing interests.

Data accessibility statement: This study produced no new data. Any data used was taken from existing publication and is detailed in the Supplementary Information.

Abstract

Changes in temperature affect consumer-resource interactions which underpin the functioning of ecosystems. However, existing studies report contrasting predictions regarding the impacts of warming on biological rates and community dynamics. To improve prediction accuracy and comparability, we develop a framework that combines two approaches: sensitivity analysis and aggregate parameters. The former determines which biological parameters impact the community most strongly. The use of aggregate parameters (i.e., maximal energetic efficiency, ρ, and interaction strength, κ), that combine multiple biological parameters, increases explanatory power and reduces the complexity of theoretical analyses. We illustrate the framework using empirically-derived thermal dependence curves of biological rates and applying it to consumer-resource biomass ratio and community stability. Based on our analyses, we present four predictions: 1) resource growth rate regulates biomass distributions at mild temperatures, 2) interaction strength alone determines the thermal boundaries of the community, 3) warming destabilises dynamics at low and mild temperatures only, 4) interactions strength must decrease faster than maximal energetic efficiency for warming to stabilise dynamics. We argue that directly measuring the aggregate parameters should increase

the accuracy of predictions on warming impacts on food webs and promote cross-system comparisons.

Introduction

Temperature strongly regulates consumer-resource interactions that constitute the fundamental blocks of ecosystems (O'Connor *et al.* 2009; Montoya & Raffaelli 2010; Petchey *et al.* 2010; Rall *et al.* 2012; Amarasekare 2019), and anthropogenic climate change will, in most cases, increase mean temperatures (*IPCC 2013*). Therefore, understanding and predicting the impacts of warming on consumer-resource interactions has attracted much interest, particularly over the past two decades (Vasseur & McCann 2005; Binzer *et al.* 2012; Thakur *et al.* 2017). A major breakthrough occurred with the postulation that metabolic rate increases exponentially with temperature, with the slope (often referred to as activation energy) conserved across levels of organisation (Gilooly *et al.* 2001; Brown *et al.* 2004). However, activation energies can vary significantly among organisms and between different biological rates (Dell *et al.* 2011; Réveillon *et al.* 2019). In addition, the thermal response curve of certain biological rates has been shown to decrease at high temperatures, producing a unimodal thermal dependence shape (Deutsch *et al.* 2008; Pörtner & Farrell 2008; Englund *et al.* 2011; Uiterwaal & DeLong 2020). This lack of consensus regarding the exact shape of the temperature-dependence of physiological rates (e.g. ingestion rates), behavioural traits (e.g. consumer search or attack rates) or production (carrying capacity) has contributed to diverging, sometimes contradicting, predictions of how consumer-resource interactions will respond to warming (e.g. Vucic-Pestic *et al.* 2011; Sentis *et al.* 2012).

A dual approach to address the divergence in predictions

Two community properties which describe important features of the community are consumer-resource biomass ratio and stability, defined with respect to the occurrence of oscillations. Their importance is reflected in their prevalence in the literature on the effects of warming on consumer-resource communities and food webs (Rall *et al.* 2010, 2012; Uszko *et al.* 2017; Barbier & Loreau 2019; Bideault *et al.* 2020). However, predictions vary about the impacts of warming on both these community properties. Biomass ratios have been theorised to increase (Vasseur & McCann 2005; Rip & McCann 2011; Gilbert *et al.* 2014) or decrease (Vasseur & McCann 2005) monotonically with warming, though experimentally-derived data have mainly yield unimodal responses (Fussmann *et al.* 2014; Uszko *et al.* 2017). Likewise, the effects of warming on stability remain unclear. Using data on specific rates (e.g. attack, ingestion and metabolic rates), studies have inferred that stability either increases monotonically (Rall *et al.* 2010, 2012; Vucic-Pestic *et al.* 2011; Fussmann *et al.* 2014) or responds unimodally (Sentis *et al.* 2012; Betini *et al.* 2019) to warming. Theoretical work on stability, in particular on the mechanisms causing the onset of oscillations, expands decades (Rosenzweig & MacArthur 1963; Rosenzweig 1971; May 1972). Vasseur and McCann (2005) used a temperature-dependent bioenergetic model to show that warming will destabilise consumer-resource communities when the consumer metabolic rate increases faster than the ingestion rate. More recently, Johnson and Amarasekare (2015) pointed out the pivotal role of the temperature-dependence of carrying capacity — rather than metabolism and ingestion — in determining warming-stability relationships. All these examples highlight that the mixed predictions, whether empirically-derived or theoretical, originate from two distinct sources: the different parameters hypothesised to be driving community responses and the thermal dependence shapes of these parameters. Therefore, to improve the accuracy of predictions regarding the effects of warming on consumer-resource communities, we need to establish which biological

parameters drive community properties (e.g. biomass distribution, stability) and to acquire a better mechanistic understanding of how their thermal dependence shapes affect community properties.

A dual approach utilising sensitivity analysis and the application of aggregate parameters can address both these issues (Fig. 1). On the one hand, a sensitivity analysis will establish the parameters that most strongly influence the community property of interest (e.g. biomass distribution, stability). A sensitivity analysis quantifies the incremental rate of increase in a response variable with respect to an incremental increase in a parameter. It has been extensively used in population ecology and demography (Caswell 2019), with important applications in applied ecology (Manlik *et al.* 2018). Since the relative importance of parameters can change along the temperature gradient and consumer-resource communities will be subjected to warming, a sensitivity analysis allows us to determine the temperatures at which different parameters have the strongest relative impact (Zhao *et al.* 2020).

On the other hand, we can aggregate groups of the primary parameters into fewer, biologically meaningful and empirically measurable quantities. The use of such aggregate parameters would reduce the complexity of theoretical analyses, provide a mechanistic interpretation for the difference in predictions and facilitate the comparison among predictions. Experimentally, replacing multiple measurements of individual parameters with measurements of the aggregates could also restrict the room for divergent findings. Aggregate parameters have been utilised in theoretical studies already (Barbier & Loreau 2019; Bideault *et al.* 2020). The seminal paper of Yodzis and Innes (1992) reduced the analysis of consumer-resource interactions to two principal aggregate parameters; consumer maximal energetic efficiency and a measure of resource abundance. A variation of maximal energetic efficiency (termed

energetic efficiency) has been widely used by empirical studies; however, rather than being measured directly, its value has been derived from the measurements of its principle components, i.e., feeding and metabolic rates (Rall *et al.* 2010; Vucic-Pestic *et al.* 2011; Sentis *et al.* 2012). Gilbert et al. (2014) posited that a single aggregate parameter — interaction strength defined as the impact of the consumer on the resource population density — could capture the effects of warming on the stability of consumer-resource interactions. However, their approach was based on a type I (non-saturating) functional response, which is not a realistic assumption as most consumer-resource species pairs produce type II or III saturating functional responses (Jeschke *et al.* 2004). Moreover, the thermal dependence of interaction strength and the dominant eigenvalue (i.e., a measure of stability) were shown to not correlate well for type II or III functional responses (Uszko *et al.* 2017), pointing to a more complex relationship between interaction strength, warming and stability. We propose the use of two aggregate parameters, both of which have been independently explored in the literature. These are the maximal energetic efficiency of the consumer population, defined as the ratio of energetic gains through ingestion with no resource limitation (i.e., maximal energetic gains) over energetic losses associated to metabolic demand (Yodzis & Innes 1992) and interaction strength, measured as the ratio of resource population density without consumers to resource population density with consumers (Gilbert *et al.* 2014).

Thus, our dual approach framework identifies the parameters whose thermal dependencies drive divergence in predictions through the sensitivity analysis and simplifies complex theoretical explorations and empirical measurements through the two aggregate parameters (Fig. 1). By expressing the sensitivities and the community dynamics in terms of the aggregate parameters, analyses collapse into two dimensions. This creates a simple and mechanistic tool which will facilitate the advancement, increase the accuracy and improve comparability of

theoretical and empirically-driven predictions on the impact of warming on consumer-resource communities. Our framework can be applied to both static and dynamic properties of the consumer-resource interactions. We illustrate this application using consumer-resource biomass ratio and a stability metric quantifying the proximity to oscillations, respectively; these two variables dominating the literature on the effects of warming on consumer-resource communities and food webs (Vasseur & McCann 2005; Rall *et al.* 2008; Vucic-Pestic *et al.* 2011; Uszko *et al.* 2017; Betini *et al.* 2019). We implement different thermal parameterisations from the literature to elucidate how the relative importance of different parameters and their varying thermal dependence shapes impact predictions about the effects of warming on consumer-resource interactions. Based on our results, we make four predictions which can be theoretically and empirically tested.

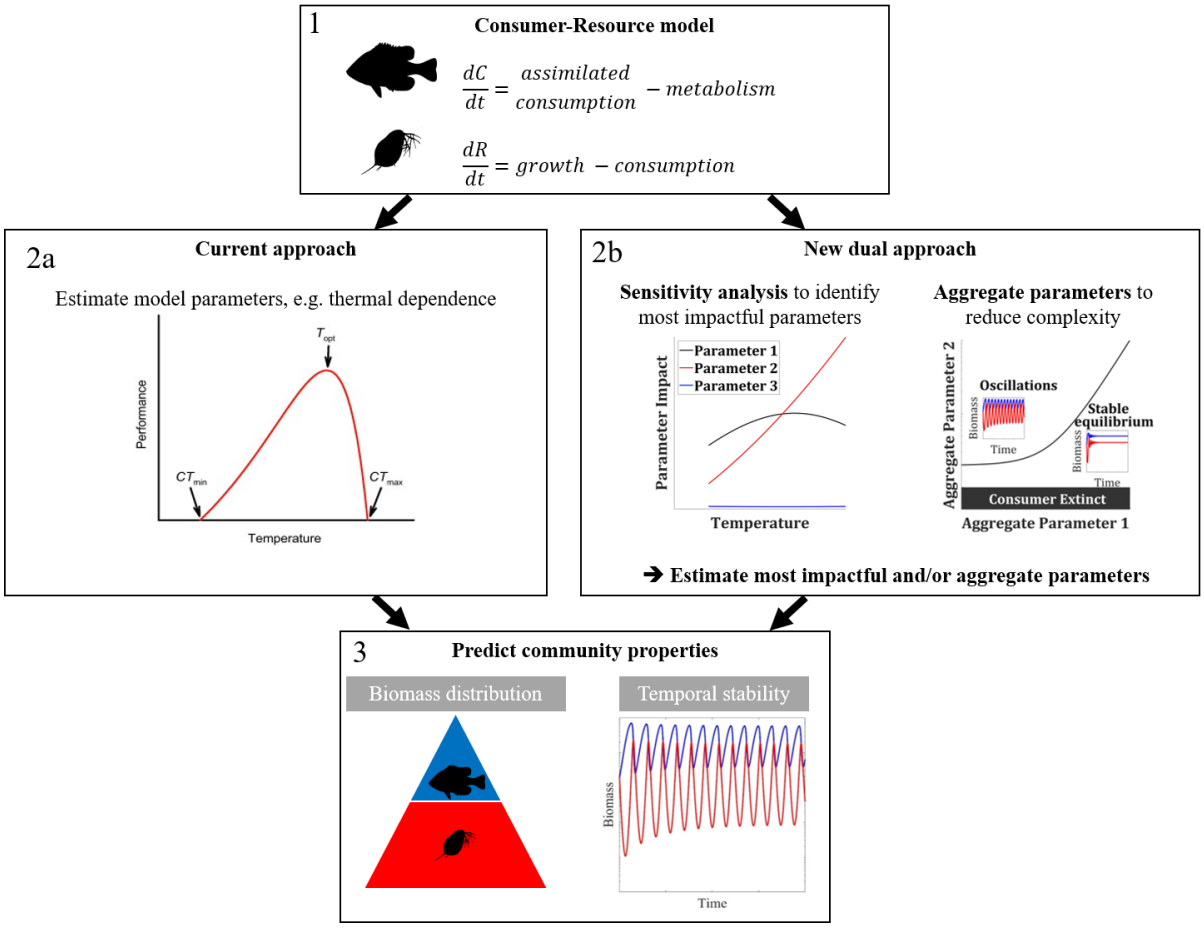

Figure 1. Illustration of the current and new dual approaches to predict the impact of global change drivers on community properties. 1) Predictions require a consumer-resource model; the Rosenzweig-MacArthur model (Rosenzweig & MacArthur 1963) or its bioenergetic equivalent (Yodzis & Innes 1992) have been used most commonly. 2a) The current approach is to experimentally estimate parameters which are considered significant (e.g. consumer feeding and metabolic rates for warming-stability relationships) to parameterise the model. Assuming the remaining parameter values, the model is then used to produce predictions. 2b) Our new dual framework combines two approaches to increase the accuracy of predictions and facilitate their comparison. First a sensitivity analysis determines which parameters have the greatest relative impact on the community property of interest along the environmental gradient. Then, aggregate parameters which represent biologically measurable quantities are used to express all sensitivities and determine the stability dynamics. Collapsing analyses to the two aggregate parameters reduces complexity and increases mechanistic tractability. 3) Through the empirical determination of the most appropriate parameters and the reduction in the number of measurements required, prediction accuracy improves. The advantages of the new dual approach are twofold. First, as the sensitivity analysis will have identified the most impactful parameters, the source of divergence in predictions can be isolated. Second, the aggregates represent standardised measurable population-level indicators across systems, making predictions directly comparable.

Framework construction

We used the Rosenzweig-MacArthur model (Rosenzweig & MacArthur 1963) describing the rate of change in resource and consumer biomass densities:

$$\frac{dR}{dt} = r(1 - \frac{R}{K})R - \frac{aR}{1+ahR}C \quad (1)$$

$$\frac{dC}{dt} = (e\frac{aR}{1+ahR} - m)C \quad (2)$$

R is the resource species biomass density and C the consumer species biomass density. Here we present density with respect to volume [$\frac{g}{m^3}$], but densities can also be with respect to area [$\frac{g}{m^2}$], which would require an adjustment for certain parameters' units (Supplementary Information, SI 1). Resource growth is assumed to be logistic, with an intrinsic growth rate r [$\frac{1}{d}$] and carrying capacity K [$\frac{g}{m^3}$]. Resource biomass density is limited by the consumer through a saturating Holling type II functional response with consumer attack rate a [$\frac{m^3}{gd}$] and handling time, h [d]. Consumer growth is proportional to the assimilated consumed biomass, with e the dimensionless assimilation efficiency, while losses occur due to metabolic costs, m [$\frac{1}{d}$]. We chose a type II response due to its prevalence in many natural consumer-resource interactions (Jeschke *et al.* 2004). However, our approach was not confined to type II functional responses, as we demonstrated by applying it to the general form of the functional response (SI 1). Similarly, we represented the functional response, $f(R) = \frac{aR}{1+ahR}$, in terms of attack rate and handling time, but our approach can be easily transferred to the formulation with maximum consumption rate, J, and half-saturation density, R_0, $f(R) = \frac{JR}{R_0+R}$ (SI 2).

Aggregate parameters and stability

A characteristic feature of the Rosenzweig-MacArthur model is the appearance of population cycles (oscillations) with increasing productivity (i.e., carrying capacity) or energy fluxes more

generally (Rip & McCann 2011); the former commonly known as the 'paradox of enrichment' (Rosenzweig 1971). Therefore, the coexistence equilibrium can be stable or unstable, where dynamics oscillate around the unstable equilibrium (i.e., a limit cycle). The point at which the equilibrium switches from stable to unstable is termed a Hopf bifurcation. Theoretical studies have focused on this qualitative change to address stability (Yodzis & Innes 1992; Vasseur & McCann 2005; Amarasekare 2015) because these distinct regimes translate to different temporal dynamics, with oscillations leading to greater variability over time. Hence, we applied a stability metric that quantifies the tendency of the dynamics to oscillate (Johnson & Amarasekare 2015).

For our analyses we assumed dynamics had either converged to the stable equilibrium or the limit cycle. We, therefore, started by determining the coexistence equilibria analytically in order to derive the population biomass densities that we used to calculate the biomass ratio. Equilibrium implies a zero rate of change for both consumer and resource biomass densities. In the case of the limit cycle, this yields the unstable equilibrium which is approximately equal to the time-averaged values along the limit cycle. Thus, we set equations (1) and (2) equal to zero and solved the system of equations to yield the coexistence equilibrium:

$$R_S = \frac{m}{a(e-mh)} \qquad (3)$$

$$C_S = er\frac{aK(e-mh)-m}{a^2K(e-mh)^2} \qquad (4)$$

And the biomass ratio:

$$\mathcal{B} = \frac{C_S}{R_S} = er\frac{aK(e-mh)-m}{amK(e-mh)} \qquad (5)$$

Biologically meaningful values require that R_S and C_S are positive, which yielded two conditions for coexistence:

$$e - mh > 0 \qquad (6)$$

$$aK(e - mh) - m > 0 \qquad (7)$$

If (6) fails, i.e., $e - mh < 0$, then (7) cannot be satisfied because $aK(e - mh) > m$ will be impossible (all parameters are required to have positive values). Therefore, if (7) holds, it necessarily implies that (6) is also satisfied. Hence (7) is a necessary and sufficient condition for coexistence.

Finally, the Hopf bifurcation occurs when the eigenvalues cross zero. This condition can be reduced to following expression:

$$ahK(e - mh) - e - mh = 0 \qquad (8)$$

Similar to Yodzis and Innes (1992) and Vasseur and McCann (2005), we represented the coexistence boundaries (eq. 6 and 7) as well as the Hopf bifurcation (eq. 8) through two aggregate parameters to reduce the complexity of the analyses, collapsing the problem from six to two dimensions. We selected maximal energetic efficiency, $\rho = \frac{e}{mh}$, and interaction

strength, $\kappa = ahK\left(\frac{e}{mh} - 1\right)$. A closer look at the aggregate parameters ρ and κ elucidates their biological meaning.

$\frac{1}{h}$ is the saturation value of the functional response and thus represents the maximum consumption rate, J. Hence, ρ can be written as:

$$\rho = \underbrace{e}_{\substack{consumer \\ assimilation \\ efficiecny}} * \underbrace{J}_{\substack{maximum \\ consumption\ rate}} * \underbrace{\frac{1}{m}}_{\substack{consumer \\ metabolic \\ loss}} = \frac{maximal\ energetic\ gain}{energetic\ loss}$$

ρ measures the net energetic gain of the consumer population biomass assuming its maximum feeding rate is realised. This occurs under conditions of no resource limitation, when the functional response has saturated, hence the term maximal energetic efficiency. ρ was introduced by Yodzis and Innes (1992) and considered a key aggregate parameter to understand food web dynamics. In empirical studies, a variant of ρ termed energetic efficiency, y, has been often applied (Rall *et al.* 2010; Sentis *et al.* 2012, 2017). Unlike ρ, y is a function of the full functional response term and hence also depends on resource density, $y = \frac{e*f(R)}{m}$, where $f(R) = \frac{aR}{1+ahR}$ at a specified resource density, R.

Expanding and then simplifying the second aggregate parameter κ produced:

$$\kappa = ahK\left(\frac{e}{mh} - 1\right) = \frac{aK(e - mh)}{m} = \frac{K}{R_S}$$

Therefore, κ is the ratio of the resource equilibrium density without consumers (the carrying capacity) to the resource equilibrium density with consumers. This quantifies the effect of the consumer population on the resource population, hence κ represents interaction strength in the community (Berlow *et al.* 1999; Gilbert *et al.* 2014).

By substituting ρ and κ into eq. 6 and 7, these became:

$$\rho > 1 \qquad (9)$$

$$\kappa > 1 \qquad (10)$$

Now, eq. (10) represents the necessary and sufficient condition for coexistence and hence determines the feasibility boundary of the community.

Similarly, eq. 8 becomes:

$$\kappa - \rho - 1 = 0 \qquad (11)$$

Therefore, whether the equilibrium is stable or unstable can be determined exclusively in terms of ρ and κ (eq. 11). As a metric to determine stability, we used the one proposed by Johnson and Amarasekare (2015) by expressing it in terms of ρ and κ and adjusting it so that it vanished at the Hopf bifurcation (SI 3). This metric, $\mathcal{S}$, quantifies stability solely in relation to the Hopf bifurcation.

$$\mathcal{S} = -\frac{(\kappa-\rho-1)}{\rho-1} \qquad (12)$$

$\mathcal{S} > 0$ corresponds to a stable equilibrium and $\mathcal{S} < 0$ to oscillations.

Sensitivity analysis

We performed a sensitivity analysis of the biomass ratio ($\mathcal{B}$) and the stability metric ($\mathcal{S}$) with respect to the original model parameters (i.e., r, K, a, h, e and m). Generally, a sensitivity analysis quantifies the effect of a change in a parameter on the response variable of choice. It is important to note that while one parameter is being perturbed, all others are assumed to remain constant. Different types of sensitivity indices exist such as simple sensitivity and elasticity (Manlik *et al.* 2018; Caswell 2019). Here we used elasticity for biomass ratio ($\mathcal{B}$) and an adjusted elasticity for stability ($\mathcal{S}$), to avoid values diverging towards infinity close to the Hopf bifurcation.

Elasticity is a proportional sensitivity, quantifying how a relative change in a parameter translates into a relative change in the variable; otherwise known as the log-scaled sensitivity (Manlik *et al.* 2018). Thus, the elasticity of $\mathcal{B}$ with respect to a parameter, x, is given by:

$$\partial_x \mathcal{B} = \frac{\frac{\partial \mathcal{B}}{\mathcal{B}}}{\frac{\partial x}{x}} = \frac{\partial \ln(\mathcal{B})}{\partial \ln(x)} \quad (13)$$

Therefore, $\partial_x \mathcal{B} = 1$ means that a relative increase of 10% in parameter x causes a relative increase of 10% in variable $\mathcal{B}$. Conversely, $\partial_x \mathcal{B} = -1$ implies that a relative increase of 10% in parameter x results in relative decrease of 10% in $\mathcal{B}$.

For the sensitivity of the stability metric, $\mathcal{S}$, we used a variation of the elasticity because $\mathcal{S}$ approaches zero close to the Hopf bifurcation. Hence, calculating the relative change in $\mathcal{S}$ would cause elasticities to diverge towards infinity. Therefore, we defined the sensitivity of $\mathcal{S}$ as the incremental change in $\mathcal{S}$ induced by a relative change in parameter x.

$$\partial_x \mathcal{S} = \frac{\partial \mathcal{S}}{\frac{\partial x}{x}} = \frac{\partial \mathcal{S}}{\partial \ln(x)} \qquad (14)$$

In this way, $\partial_x \mathcal{S} = 1$ implies that a relative increase in parameter x of 10% translates into an absolute increase of 0.1 in $\mathcal{S}$, and hence has a stabilising effect. If, conversely, $\partial_x \mathcal{S} = -1$, the same relative increase in x would lead to decrease of 0.1 in $\mathcal{S}$, corresponding to a destabilising effect.

From the above examples, it becomes clear that the magnitude and sign of each sensitivity determine how strongly and in what direction the parameter perturbation impacts the variable, respectively. Hence, we used the magnitudes to compare the parameter sensitivities and rank their relative importance. The sign provided qualitative information regarding the direction of change (increasing or decreasing the response variable).

All sensitivities could be expressed in terms of the aggregate parameters. Using these analytical sensitivity expressions, the conditions ranking the relative impact of parameters (i.e., ranking the magnitudes of all elasticities) could be represented as functions of ρ and κ. We plotted these functions in a plane with ρ and κ as axes, creating a $\rho - \kappa$ plane divided into regions of different parameter sensitivity rankings. The positions of these regions in the plane remain fixed irrespective of the parameterisation used, because the sensitivity expressions stem from the model equations and depend on the variable of the sensitivity analysis (i.e., biomass ratio

or stability in our study). The $\rho - \kappa$ plane provides additional information, such as the feasibility boundary (eq. 10) and the position of the Hopf bifurcation (eq. 11).

Temperature dependencies and parameterisations

To this point, our approach had been determined by the model equations and the single assumption that all parameters are positive as they represent biological quantities. To apply our methodology to the overarching topic of the impacts of warming on consumer-resource interactions and to demonstrate the impacts of different thermal dependencies of parameters, we implemented temperature parameterisations from the literature.

Maintenance respiration rates, m, have been shown to increase exponentially with temperature (Brown *et al.* 2004), and the Arrhenius equation is most often used to describe the thermal dependency of m (Vasseur & McCann 2005; Sentis *et al.* 2017; Uszko *et al.* 2017). However, the thermal response curves of resource growth rate, r, attack rate, a, and handling time, h, have been represented either through the Arrhenius equation (Vasseur & McCann 2005; Binzer *et al.* 2016) or as unimodal functions (Amarasekare 2015; Uszko *et al.* 2017; Zhang *et al.* 2017; Uiterwaal & DeLong 2020; Zhao *et al.* 2020). Carrying capacity, K, and consumer assimilation efficiency, e, have a less clear connection to temperature (Uszko *et al.* 2017; Dee *et al.* 2020). We selected two parametrisations related to the ongoing debate surrounding the importance of including the decreasing part of the biological rates beyond the optimal temperature (Pawar *et al.* 2016) and used these as an illustrative comparison. We thus chose one model with the unimodal parameterisation for r, a and h, the Arrhenius equation for m, and temperature-independence for K and e (Uszko *et al.* 2017). We refer to this as the 'unimodal' parameterisation. We compared this to a 'monotonic' parameterisation where all thermal

dependencies (r, a, h, K, m) follow the Arrhenius equation and e is a constant (Fussmann *et al.* 2014). Following this comparison, we plotted four additional parameterisations from the literature onto the $\rho - \kappa$ plane to broaden the comparative picture and demonstrate the simplicity of applying the framework to empirically-derived measurements. These consisted of two monotonic parameterisations (Vucic-Pestic *et al.* 2011; Binzer *et al.* 2016), one where only a was unimodal (Sentis *et al.* 2012) and one which though monotonic, did include some distinctive thermal dependencies – increasing $K(T)$ and $e(T)$ and no thermal dependence of h (Archer *et al.* 2019). We provide a description of the studies and details of their parameterisations in the supplementary material (SI 4).

We should note here that not all parameterisations included the resource growth rate, r, so the biomass ratio could not be calculated in these cases. However, we could calculate ρ and κ for all parameterisations and, as we noted above, biomass ratio elasticities are functions of ρ and κ. Therefore, plotting these thermal parameterisations on the $\rho - \kappa$ plane determined how biomass ratio sensitivities to individual parameters changed with warming regardless of the actual biomass ratio values. This meant that we could include studies which had not measured resource growth or estimated the biomass ratio to broaden the scope of the comparison of the biomass ratio sensitivities. Though this does not represent an exhaustive list of parameterisations, we were restricted to parameterisations which could be used to parametrise the Rosenzweig-MacArthur model with a type II response and whose available parameters could yield ρ and κ. For each parameterisation, we determined a feasible temperature range, where the resource and consumer had non-negative biomass densities. When we refer to 'mild' and 'extreme' temperatures, as well as 'close' or 'far' from consumer extinction, this is relative to each parameterisation's temperature range and feasibility boundaries, respectively. As outlined above, the feasible temperature range was effectively constrained by the consumer

energetic demands (i.e., κ >1) with the temperature extremes corresponding to the point of consumer extinction.

Similar sensitivity patterns for biomass ratio and stability

Table 1. Sensitivities of the biomass ratio ($\partial_x \mathcal{B}$) and of the stability metric ($\partial_x \mathcal{S}$) with respect to the six original model parameters. All sensitivities are expressed in terms of ρ and κ.

Parameter	Consumer-resource biomass ratio, $\mathcal{B}$	Stability metric, $\mathcal{S}$
x	$\partial_x \mathcal{B} = \frac{\partial \ln(\mathcal{B})}{\partial \ln(x)}$	$\partial_x \mathcal{S} = \frac{\partial \mathcal{S}}{\partial \ln(x)}$
r	1	0
K	$\frac{1}{\kappa - 1}$	$-\frac{\kappa}{\rho - 1}$
a	$\frac{1}{\kappa - 1}$	$-\frac{\kappa}{\rho - 1}$
h	$-\frac{1}{(\rho - 1)(\kappa - 1)}$	$\frac{\kappa(1-\rho) + 2\rho}{(\rho - 1)^2}$
e	$\frac{\rho}{(\rho - 1)(\kappa - 1)} + 1$	$-\frac{2\rho}{(\rho - 1)^2}$
m	$-\frac{\rho}{(\rho - 1)(\kappa - 1)} - 1$	$\frac{2\rho}{(\rho - 1)^2}$

Biomass ratio: always most sensitive to e and m

We analytically obtained four groups of biomass ratio elasticity magnitudes, $\partial_e \mathcal{B} = |\partial_m \mathcal{B}|$, $\partial_K \mathcal{B} = \partial_a \mathcal{B}$, $\partial_r B$ and $\partial_h \mathcal{B}$. e and m always have the largest elasticity magnitude and hence the

strongest relative impact on the biomass ratio ($\partial_e\mathcal{B}, |\partial_m\mathcal{B}| > \partial_K\mathcal{B}, \partial_a\mathcal{B}, |\partial_h\mathcal{B}|, \partial_r\mathcal{B}$, Table 1). $\partial_e\mathcal{B} > 0$ and $\partial_m\mathcal{B} < 0$, so increasing e increases the biomass ratio, while increasing m reduces it. K and a have equal and positive elasticities ($\partial_K\mathcal{B} = \partial_a\mathcal{B} > 0$), both increasing the biomass ratio. The elasticity of r is constant, $\partial_r\mathcal{B} = 1$, meaning that a relative increase of e.g. 10% in parameter r, causes a relative increase of 10% in $\mathcal{B}$. Finally, $\partial_h\mathcal{B} < 0$, meaning that increases in h reduce the biomass ratio. These are general results, which hold independently of any model parameterisation (with temperature or otherwise) and follow directly from the Rosenzweig-MacArthur model's equations.

Biomass ratio: high r elasticity far from thermal boundaries

Both the 'unimodal' and 'monotonic' temperature parameterisations (see Framework construction, *Temperature dependencies and parameterisations*), produced a unimodal biomass ratio thermal dependence (Fig. 2). The unimodal parameterisation induced thermal boundaries to the community at both low (1°C) and high (33°C) temperatures (Fig. 2a). The biomass ratio peaked at 14°C around $\mathcal{B} \approx 5.5$; it exceeded 1 for most temperatures (implying higher consumer than resource biomass) and decreased rapidly to 0 as it approached both thermal boundaries (low and high temperature extremes). The biomass ratio of the monotonic parameterisation increased with warming from low temperatures, peaked at 0.19, before decreasing to 0 (Fig. 2b), as consumers became extinct at high temperatures (27.5°C). We should remark that the two parameterisations are derived from different systems and as such have different temperature ranges.

In both parameterisations, sensitivity to e and m was highest throughout (Fig. 2c, d) - as expected based on the analytical findings. Sensitivity to r was second highest for most

temperatures. Sensitivities were split into two groups at mild temperatures: e, m and r had the highest sensitivity with $\partial_e\mathcal{B} = |\partial_m\mathcal{B}| \approx \partial_r\mathcal{B} = 1$, while sensitivity to a, h and K was very low. Approaching the temperature extremes all elasticities besides $\partial_r\mathcal{B}$ diverged in both parameterisations; $\partial_h\mathcal{B}$ diverged faster than $\partial_a\mathcal{B} = \partial_K\mathcal{B}$ in the unimodal parameterisation (Fig. 2c), while the opposite occurred in the monotonic one (Fig. 2d). Thus, despite the similar pattern of diverging elasticities in both parameterisations, the elasticity rankings close to the thermal extremes differed between the parameterisations (as can be seen in the background colours of Fig. 2a and b).

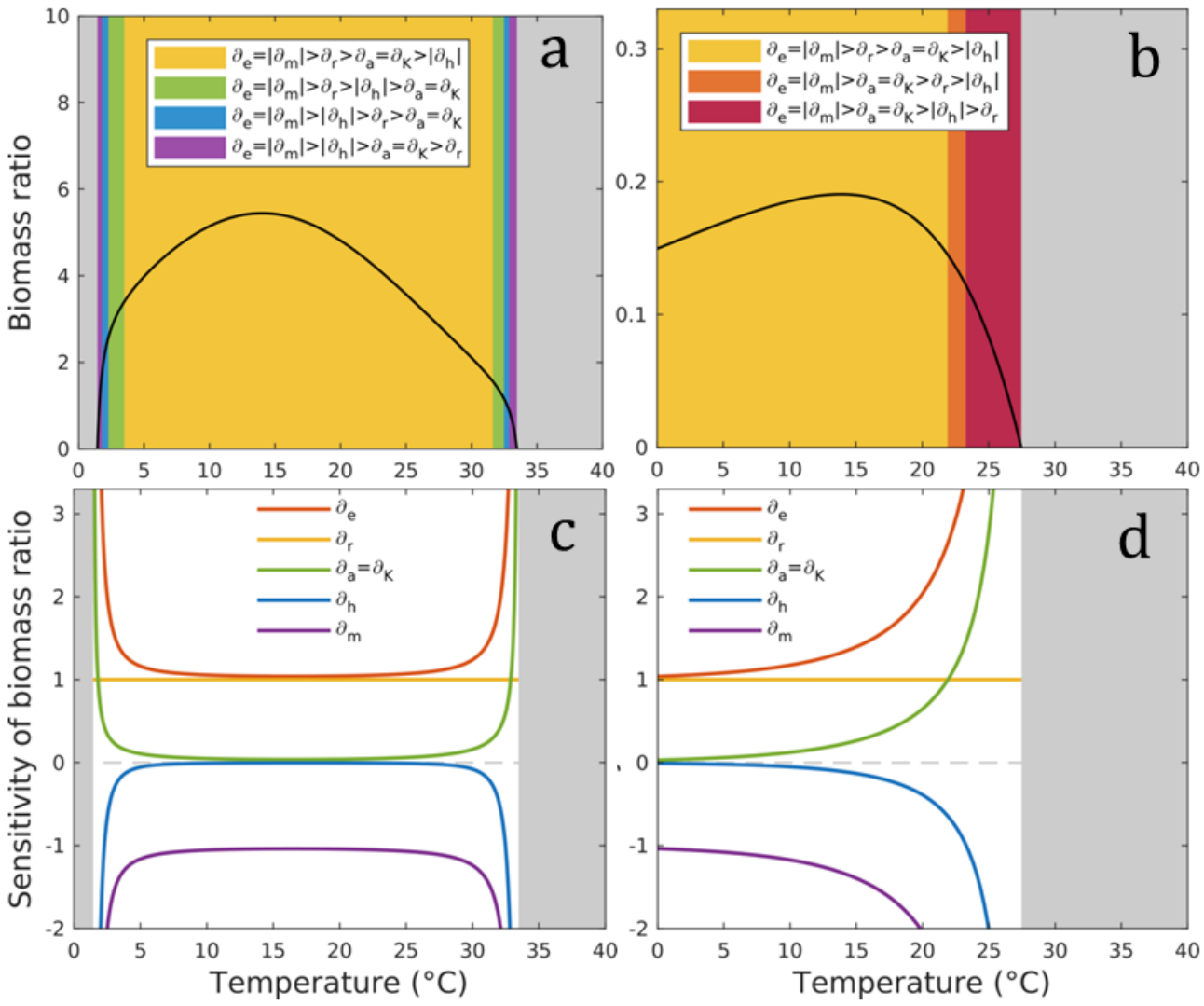

Figure 2. Consumer-resource biomass ratios for the (a) unimodal and (b) monotonic parametrisations along the temperature gradient. Feasible temperature ranges are constrained by the condition of positive biomass densities for both consumer and resource (grey areas correspond to consumer extinction). The different background colours correspond to different elasticity rankings of model parameters (see legend). Panels (c) and (d) provide the values of the six parameter elasticities along the temperature gradient for the unimodal and monotonic parameterisations, respectively.

Using the elasticity expressions in terms of ρ and κ (Table 1) reduces the comparison of the two parameterisations' elasticities to two dimensions. Ranking the elasticity magnitudes (besides $\partial_e \mathcal{B} = |\partial_m \mathcal{B}|$) of $\partial_K \mathcal{B} = \partial_a \mathcal{B}, |\partial_h \mathcal{B}|$ and $\partial_r \mathcal{B}$ requires six conditions. These create six distinct regions in the $\rho - \kappa$ plane which correspond to different elasticity ranking orderings and provide a mechanistic overview of which elasticities dominate where (Fig. 3a). Regions adjacent to consumer extinction ($\kappa = 1$) have high sensitivity to either h (purple region) or to a and K (red and orange regions). r elasticity is highest in the regions farthest from consumer extinction (green and yellow regions). Finally, the two temperature parameterisations were mapped onto this plane by calculating the corresponding ρ and κ values (Fig 3b and c). Each parameterisation yielded a unique trajectory through the regions of the $\rho - \kappa$ plane, with the two trajectories being markedly different, however both parameterisations occupied the region where r ranked second highest for most temperatures (green and yellow regions, Fig. 3b, c). The unimodal parameterisation produced a unimodal trajectory, crossing the consumer extinction threshold at low and high temperatures, passing through the regions of high h elasticity close to extinction (blue and purple regions, Fig. 3b). The monotonic parameterisation's trajectory converged monotonically towards consumer extinction with

increasing temperature, crossing the regions of high a and K elasticity prior to extinction (orange and red regions, Fig. 3c).

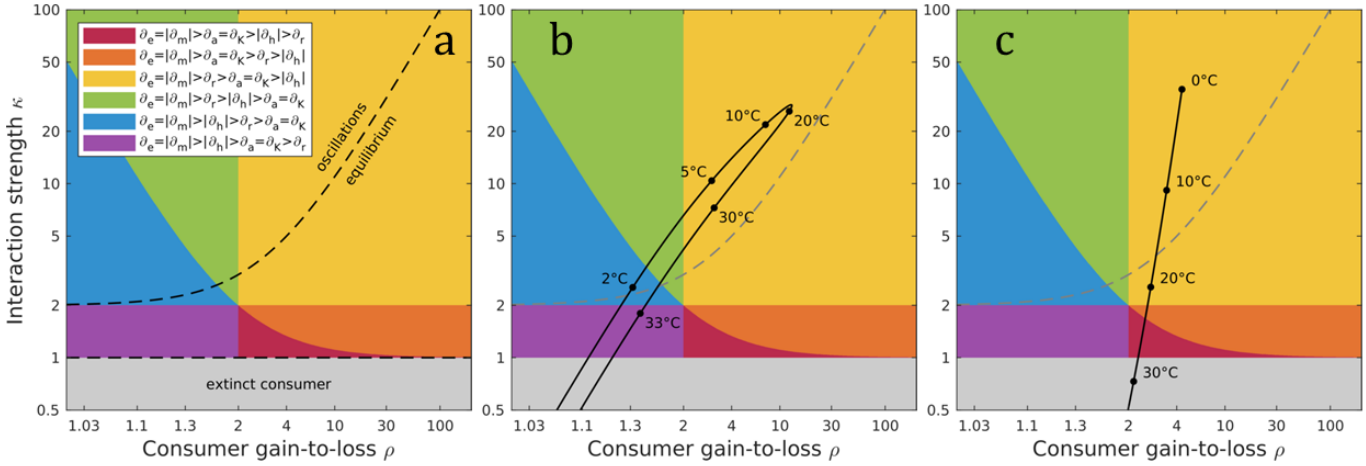

Figure 3. (a) The $\rho - \kappa$ plane split into regions of different colours corresponding to different consumer-resource biomass ratio sensitivity rankings derived from the analytic expressions (Table 1) – see legend for the relative sensitivity rankings. The plane includes the feasibility boundary ($\kappa = 1$) and the Hopf bifurcation (dotted curve splitting the plane into stable equilibrium and oscillations). The thermal dependencies of $\rho = \frac{e}{mh}$ and $\kappa = \frac{K}{R_S}$ were calculated for the (b) unimodal and (c) monotonic parameterisations yielding a trajectory for each parameterisation. The paths of the trajectories demonstrate the sensitivity regions occupied by the parameterisations.

Trajectories of the other parameterisations from the literature also occupied the region of high r elasticity for most temperatures, far from their thermal boundaries (green and yellow regions, Fig. 4). Three monotonic parameterisations produced monotonic trajectories, with extinctions only occurring at high temperatures if at all (Fig. 4a, b, c). The trajectories began in the region of high r elasticity (yellow region), converged monotonically towards consumer extinction

($\kappa = 1$), approaching or crossing the region of high a and K elasticity at high temperatures (orange and red regions). In the parameterisation where only attack rate's thermal dependence was unimodal, a unimodal trajectory emerged (Fig. 4d). At low temperatures it occupied the region of high r elasticity but moved away from consumer extinction. With further warming, the trajectory switched direction and followed the same path as the monotonic parameterisations, crossing the consumer extinction boundary via the region of high a and K elasticity (orange and red regions). In the parameterisation combining a unimodal thermal dependence for attack rate and handling time, extinctions occurred at low and high temperatures imposing a unimodal trajectory (Fig. 4e). The trajectory crossed the consumer boundary at low ρ, via the regions of high h relative importance (blue and purple regions). The final parameterisation, though monotonic, yielded unimodal trajectories (Fig. 4f). A monotonically increasing $K(T)$ (as opposed to decreasing in the other monotonic parameterisations and constant in the unimodal ones) initially forced the trajectory away from consumer extinction, while remaining in the region of high r elasticity. With warming, consumer energetic efficiency ρ decreased and the trajectory approached the resource thermal boundary ($\rho = 1$). This, in turn, pushed consumers towards extinction (see eq. 7 and 10), thus forcing an abrupt decline towards the consumer boundary, via the region of high h elasticity (blue and purple regions).

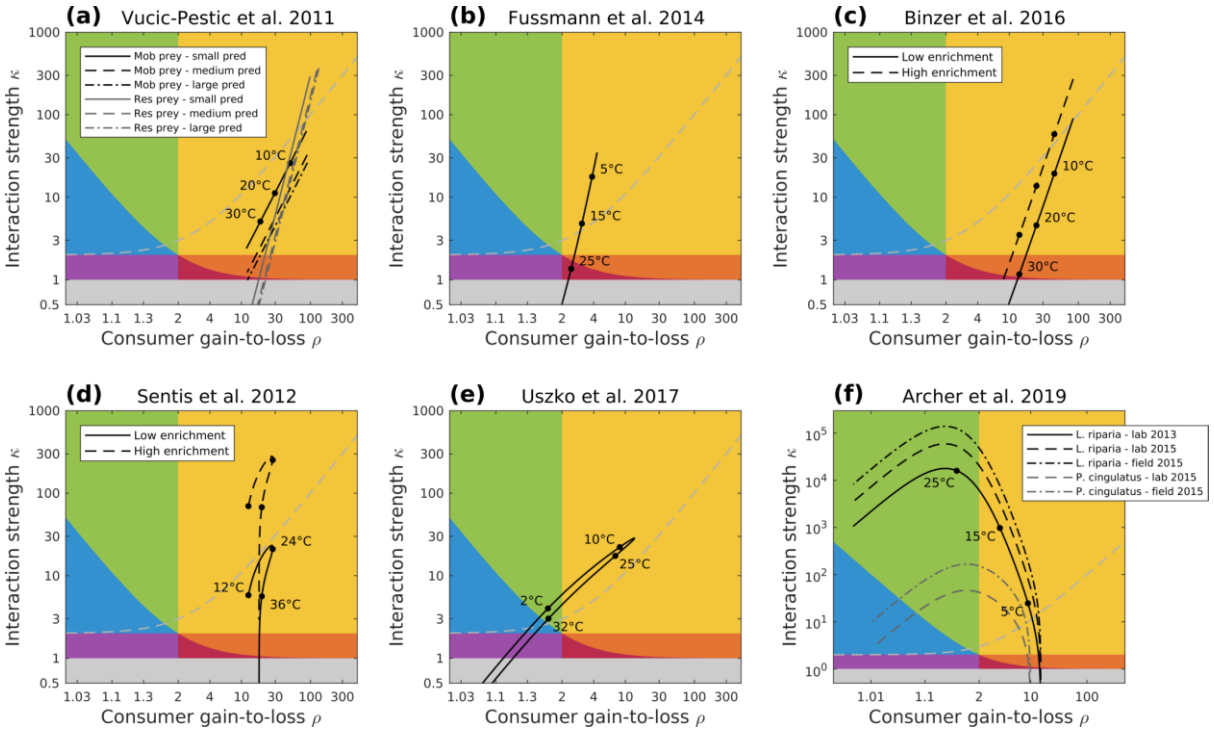

Figure 4. Trajectories of the six empirical temperature parameterisations in the $\rho - \kappa$ plane: a) Vucic-Pestic *et al.* (2011) with six different interaction experiments – three predator size-classes and two types of prey, b) Fussmann *et al.* (2014), c) Binzer *et al.* (2016) with two levels of enrichment, d) Sentis *et al.* (2012), with two levels of enrichment, e) Uszko *et al.* (2017), f) Archer *et al.* (2019) with two prey types and three measurements. (a), (b) and (c) have monotonic thermal dependences for a, h, K, m ($K(T)$ decreasing) and a constant e. (d) has a unimodal thermal performance curve for a (hump-shaped), constant e and K, monotonic h and m. (e) has a unimodal (U-shaped) h and a (hump-shaped) thermal dependence, constant e and monotonic K, m. (f) has monotonic a, K, m, e ($K(T), e(T)$ increasing) and h constant. All parameter values are detailed in SI 4. The coloured regions demonstrate the different biomass ratio sensitivity rankings (see legend in Fig. 3a). The trajectories for each parameterisation are derived from calculating the thermal dependence of $\rho = \frac{e}{mh}$ and $\kappa = \frac{K}{R_S}$ (see Framework construction, *Temperature dependencies and parameterisations* for details).

Stability most sensitive either to e and m or to a and K

Similarly to the biomass ratio, the analytical approach for the stability sensitivities yielded results conserved independently of the temperature parameterisations (Table 1): equal sensitivity magnitudes pairwise for e and m and for a and K (i.e., $|\partial_e \mathcal{S}| = \partial_m \mathcal{S}$ and $|\partial_a \mathcal{S}| = |\partial_K \mathcal{S}|$), negative stability sensitivities of e, a and K ($\partial_e \mathcal{S}, \partial_a \mathcal{S}, \partial_K \mathcal{S} < 0$) implying they destabilise dynamics, a positive sensitivity of m ($\partial_m \mathcal{S} > 0$) indicating a stabilising effect. h can be either stabilising or destabilising and r does not affect the stability regime ($\partial_r \mathcal{S} = 0$).

The unimodal temperature parameterisation exhibited oscillations ($\mathcal{S} < 0$) over most temperatures (Fig. 5a). Only at low and high thermal extremes did dynamics briefly stabilise prior to consumer extinction. The monotonic temperature parametrisation led to oscillations at low temperatures ($\mathcal{S} < 0$), crossed a Hopf bifurcation at 17°C and dynamics were stable ($\mathcal{S} > 0$) thereafter (Fig. 5b). In both cases, stability close to consumer extinction was most sensitive to consumer assimilation efficiency, e, and metabolism, m, ($|\partial_e \mathcal{S}| = \partial_m \mathcal{S}$), followed by handling time, h (Fig. 5a, b, blue background). Moving away from the thermal boundaries, attack rate, a, and carrying capacity, K, increased in relative importance, first exchanging rankings with h (green background) then moving above e and m to become the top-ranked sensitivities (yellow background). Furthest away from the thermal boundaries, stability was most sensitive to changes a and K, followed by h (orange background). Even though h did not rank highest in any temperature range, its sensitivity was a close second both at the temperature extremes (second to $|\partial_e \mathcal{S}| = \partial_m \mathcal{S}$) or furthest away from them (second to $|\partial_a \mathcal{S}| = |\partial_K \mathcal{S}|$) (Fig. 5c, d). Additionally, h switched from destabilising away at mild temperatures ($\partial_h \mathcal{S} < 0$) to stabilising ($\partial_h \mathcal{S} > 0$) close to the temperature extremes (Fig. S5.2).

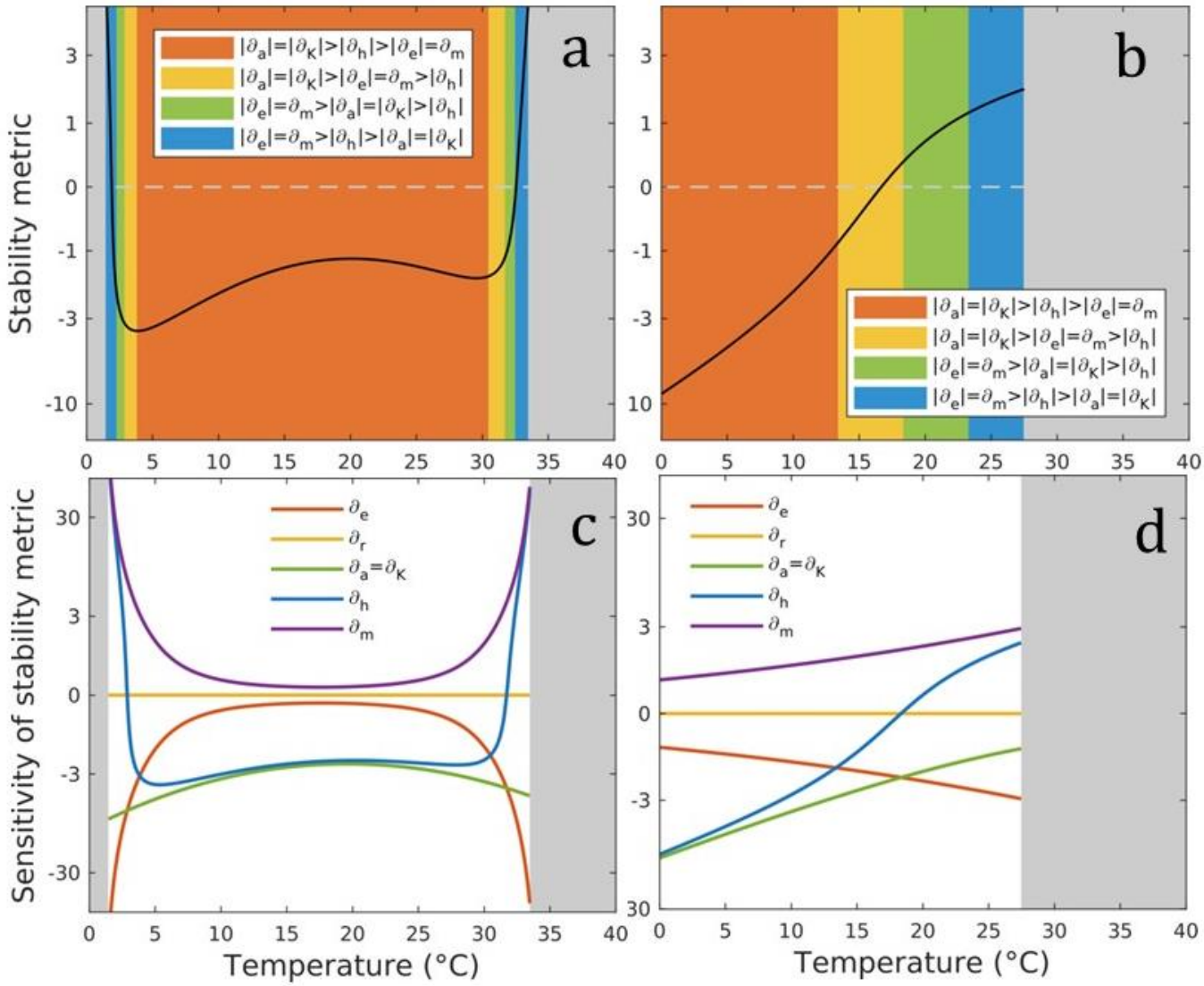

Figure 5. The thermal dependence of the stability metric, $\mathcal{S}$, for the (a) unimodal and (b) monotonic parameterisations. $\mathcal{S} > 0$ corresponds to stable dynamics, $\mathcal{S} < 0$ to oscillations. $\mathcal{S} = 0$ (dotted line) corresponds to the Hopf bifurcation. The coloured temperature ranges highlight regions of different sensitivity rankings. For temperatures beyond the community feasibility boundaries the areas are greyed out. In (c) and (d) the sensitivity to each parameter is plotted along the temperature gradient for the unimodal and monotonic parameterisations, respectively.

The $\rho - \kappa$ plane for the stability metric was split into four regions since there were three sensitivity groupings ($|\partial_e \mathcal{S}| = \partial_m \mathcal{S}, |\partial_a \mathcal{S}| = |\partial_K \mathcal{S}|, \partial_h \mathcal{S}$, while $\partial_r \mathcal{S} = 0$) and $\partial_h \mathcal{S}$ never ranked first; two regions where $|\partial_e \mathcal{S}| = \partial_m \mathcal{S}$ were the largest sensitivities (Fig. 6a, blue and green regions) and two where $|\partial_a \mathcal{S}| = |\partial_K \mathcal{S}|$ ranked highest (Fig. 6a, yellow and orange regions). The positions of the regions in the plane placed the existing results into a mechanistic context: the stability metric is most sensitive to e and m close to consumer extinction ($\kappa = 1$) and to a and K far from it. Additionally, the Hopf bifurcation (Fig. 6a, dashed curve) split the plane into stable equilibrium and oscillation regions.

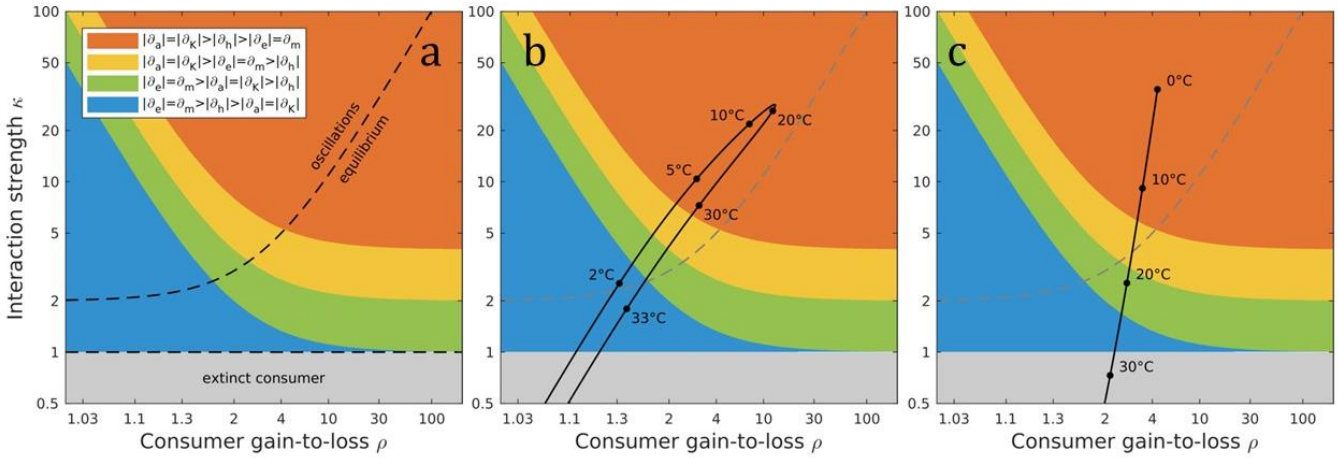

Figure 6. (a) The $\rho - \kappa$ plane split into regions of different colours corresponding to different stability sensitivity rankings derived from the analytic expressions (Table 1) – see legend for the relative sensitivity rankings. The plane includes the feasibility boundary ($\kappa = 1$) and the Hopf bifurcation (dotted curve splitting the plane into stable equilibrium and oscillations). The thermal dependencies of $\rho = \frac{e}{mh}$ and $\kappa = \frac{K}{R_S}$ were calculated for the (b) unimodal and (c) monotonic parameterisations yielding a trajectory for each parameterisation. The paths of the trajectories demonstrate the stability regime and the stability sensitivity of the parameterisations.

Corresponding to the general findings, stability in the two reference ('unimodal' and 'monotonic') parameterisations was most sensitive to changes in e and m at the thermal extremes - close to consumer extinction - and to a and K at milder temperatures – far from consumer extinction (Fig. 6b, c). The unimodal trajectory occupied the region of oscillations for most temperatures, crossing the Hopf bifurcation twice close to consumer extinction, once at low and once at high temperatures (Fig. 6b, blue region). The monotonic trajectory started in the region of oscillations and moved into the stable region with warming, crossing the Hopf bifurcation far from the thermal extreme (Fig. 6c, yellow region).

Plotting the other temperature parameterisations' trajectories onto the $\rho - \kappa$ plane reproduced the same patterns with respect to the stability metric's sensitivity (Fig. 7): stability was most sensitive to e and m at the thermal extremes and to a and K far from the extremes. The trajectories also revealed the significance of the thermal dependence shape of individual parameters on the warming-stability relationship. In three monotonic parameterisations, warming stabilised the dynamics (Fig. 7 a, b, c). In the cases, when oscillations did take place, these occurred at low temperatures (Fig 7a resident prey, b, c) and dynamics crossed the Hopf bifurcation far from the thermal boundary (orange or yellow regions). In the case with two enrichment levels (Fig. 7c), the high enrichment scenario required higher temperatures to stabilise the dynamics. In the unimodal trajectory with a unimodal thermal dependence of a (Fig. 7d), warming at low temperatures pushed the dynamics towards (low enrichment) or deeper into (high enrichment) the region with oscillations (i.e., destabilised dynamics). However, further warming caused a switch of direction in the trajectory. Subsequently, both ρ and κ decreased, with κ declining at a much faster rate, forcing the dynamics towards the stable region and eventually to consumer extinction. Both the switch in the trajectory direction and the Hopf bifurcation (high enrichment scenario) occurred at mild temperatures, in the region

of high a and K sensitivity (orange region). Here too, the destabilising impact of a high enrichment was evident. In the parameterisation with both a and h unimodal (Fig. 7e), the Hopf bifurcation occurred close to the thermal boundaries, where κ increased (low temperatures) or decreased (high temperatures) much faster than ρ. The dynamics were oscillatory for most temperatures, with the switch in the trajectory's direction occurring in the region of highest sensitivity to a and K. The final parameterisation's trajectories were characterised by a negative relationship between ρ and κ (Fig. 7f). Driven by the positive thermal dependence of carrying capacity, warming increased κ and destabilised dynamics. The trajectory crossed the Hopf bifurcation in the region of high a and K sensitivity (orange region) and dynamics oscillated for most temperatures.

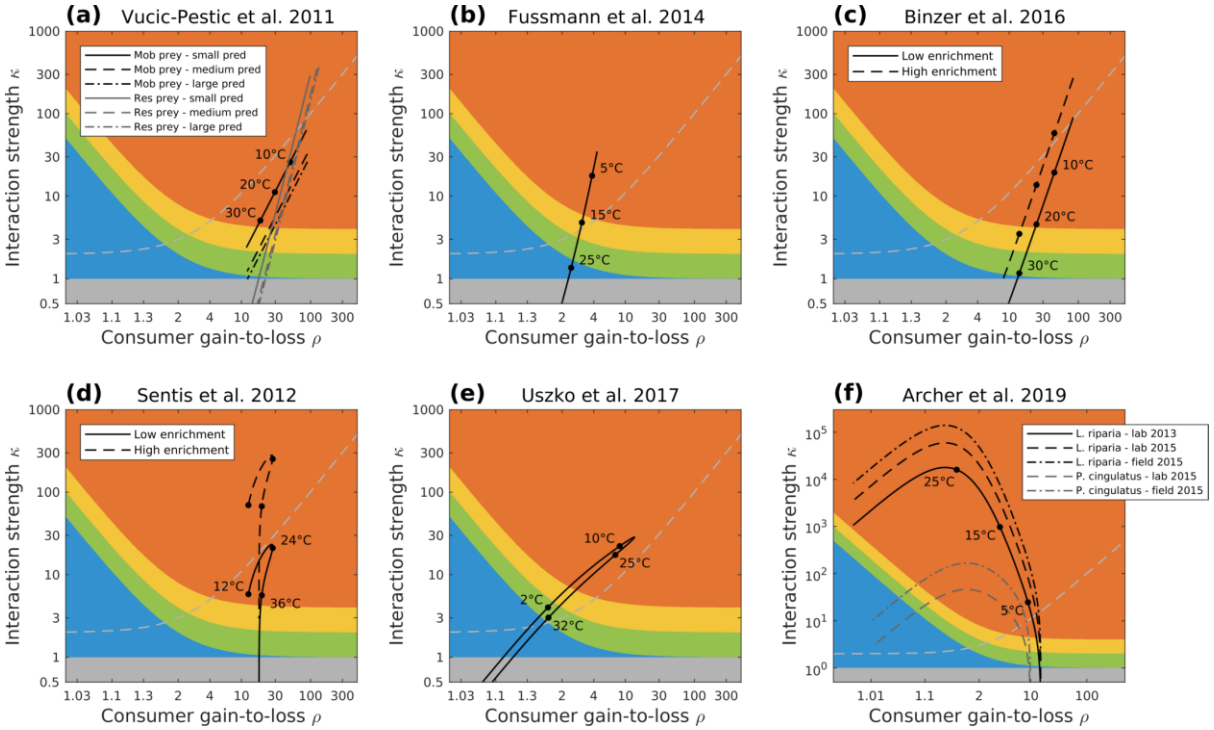

Figure 7. Trajectories of the six empirical temperature parameterisations in the $\rho - \kappa$ plane: a) Vucic-Pestic *et al.* (2011) with six different interaction experiments – three predator size-classes and two types of prey, b) Fussmann *et al.* (2014), c) Binzer *et al.* (2016) with two levels of enrichment, d) Sentis *et al.* (2012), with two levels of enrichment, e) Uszko *et al.* (2017), f)

Archer *et al.* (2019) with two prey types and three measurements. (a), (b) and (c) have monotonic thermal dependences for a, h, K, m ($K(T)$ decreasing) and a constant e. (d) has a unimodal thermal performance curve for a (hump-shaped), constant e and K, monotonic h and m. (e) has a unimodal (U-shaped) h and a (hump-shaped) thermal dependence, constant e and monotonic K, m. (f) has monotonic a, K, m, e ($K(T), e(T)$ increasing) and h constant. All parameter values are detailed in SI 4. The coloured regions demonstrate the different biomass ratio sensitivity rankings (see legend in Fig. 6a). The trajectories for each parameterisation are derived from calculating the thermal dependence of $\rho = \frac{e}{mh}$ and $\kappa = \frac{K}{R_S}$. Therefore, trajectories do not change with the variable of interest; the sensitivity regions do.

Discussion

Research on the impacts of warming on consumer-resource interactions has yielded mixed results (Vasseur & McCann 2005; Englund *et al.* 2011; Rall *et al.* 2012; Gilbert *et al.* 2014; Uszko *et al.* 2017). Resolving this debate and improving predictions has become even more pressing as most ecosystems face increased temperatures (Easterling *et al.* 2000; Walther *et al.* 2002; Root *et al.* 2003; Parmesan 2006). Here, we developed a framework to improve and simplify predictions on the impacts of warming on consumer-resource interactions. The framework integrates two distinct pathways: (1) a sensitivity analysis to identify the key biological parameters whose variations have the largest relative impact on community properties, and (2) the use of aggregate parameters (i.e., maximal energetic efficiency, ρ, and interaction strength, κ) that combine several biological parameters to increase explanatory power. We illustrated the framework using empirically-derived thermal dependence curves of biological parameters from the literature and applying it to the consumer-resource biomass ratio and a stability metric that quantifies the propensity for oscillations (Johnson &

Amarasekare 2015). Our analyses revealed that the relative significance of different parameter groupings is determined by the proximity of the consumer to its thermal boundaries and they elucidated how differences in the shape of the thermal dependence curves of individual parameters qualitatively impact predictions. Critically, our approach demonstrated the benefit of working directly with the aggregate parameters, whether from an empirical or a theoretical perspective.

We focus our discussion on the formulation of four testable predictions arising from our results. For each prediction, we present their implications and rationale. Then, we discuss more generally how our framework allows for improving the accuracy and comparability of predictions, and we present some important subtleties of its application.

Prediction 1: Resource growth rate regulates biomass distribution at mild temperatures

Implications: The relative dominance of consumer assimilation efficiency, metabolism and resource growth rate in driving changes in biomass distributions should manifest itself in any consumer-resource community far from its feasibility boundaries, assuming these communities are well-described by the Rosenzweig-MacArthur model (Fig. 3a). Due to the agreement about the thermal dependence of metabolism (Rall *et al.* 2010; Fussmann *et al.* 2014; Uszko *et al.* 2017) and the negligible -if any- change of assimilation efficiency with warming (Dell *et al.* 2011), it is differences in the thermal performance curves of resource growth rate that will strongly impact biomass ratios. Therefore, improved predictions about the impacts of warming on biomass distributions at mild temperatures necessitate the accurate description of the thermal dependence of resource growth rate.

Reasoning: Far from the community thermal boundaries, consumer assimilation efficiency, metabolism and resource growth rate always had the greatest elasticity with an almost equal relative impact on biomass ratio ($\partial_e \mathcal{B} = |\partial_m \mathcal{B}| \approx \partial_r \mathcal{B} = 1$, Fig. 2c, d and Fig. S5.1). We showed that increasing metabolism reduced biomass ratios (Table 1, Rip & McCann 2011) and this is likely to be a universal response across ecosystems, given the positive exponential dependence of metabolism on temperature across organisms (Gilooly *et al.* 2001; Brown *et al.* 2004; Rall *et al.* 2012 but see Ehnes *et al.* 2011). Conversely, assimilation efficiency increased biomass ratios but has been widely assumed to be unaffected by temperature changes (Vasseur & McCann 2005; Sentis *et al.* 2017; Uszko *et al.* 2017), though recent studies have found it can increase with warming (Lang *et al.* 2017; Daugaard *et al.* 2019). Nevertheless, this increase is of a minor scale compared to other parameters. Increasing resource growth rate also increased the biomass ratio. However, evidence on the shape of resource growth's thermal response remains inconclusive: it can either increase exponentially with temperature (Savage *et al.* 2004) or decrease abruptly beyond the thermal optimum (Dannon *et al.* 2010; Thomas *et al.* 2012). Since the biomass ratio is directly proportional to the resource growth rate ($\partial_r \mathcal{B} = 1$, Table 1), it will be strongly affected by the values and shape of the resource growth rate thermal performance curve. Given the consensus surrounding the temperature-dependence of metabolism and the minor scale of potential change in assimilation efficiency with temperature, our findings emphasise the significance of correctly parameterising the resource growth rate when aiming to predict biomass distribution changes due to warming at mild temperatures.

Prediction 2: Interaction strength alone determines consumer survival with increasing temperatures.

Implications: Determining the thermal boundaries of the community can be simplified by measuring solely the thermal dependence of interaction strength, κ. This quantity — the ratio of the resource equilibrium density without consumers (the carrying capacity) to the resource equilibrium density with consumers — can be determined experimentally (Berlow *et al.* 2004) or through observations and would facilitate cross-system predictions and comparisons thereof.

Reasoning: Close to the consumer extinction boundary, biomass ratio sensitivities to all parameters apart from resource growth diverge (Fig. 2c, d and Fig. S5.1). Therefore, consumer survival and by extension the feasibility of the community becomes extremely sensitive to the thermal dependence of individual parameters, making accurate predictions challenging. Currently, consumer survival has been inferred through energetic efficiency — the effective energetic gain of consumers at a certain resource density, which requires determining the thermal dependence of the functional response (Vucic-Pestic *et al.* 2011; Archer *et al.* 2019). Not only is the functional response's thermal dependence hotly contested (Uszko *et al.* 2017; Uiterwaal & DeLong 2020), but this uncertainty will be exacerbated by the extremely high sensitivities at the community's thermal boundaries. We showed there exists an alternative, empirically simpler and theoretically more robust metric to determine consumer survival, and hence community feasibility. Interaction strength –the relative values of resource equilibrium without and with consumers (Berlow *et al.* 1999, 2004; Gilbert *et al.* 2014)- yields the necessary and sufficient condition for consumer survival ($\kappa > 1$, eq. 10). This provides an accurate threshold and represents a measurable quantity that can be standardised across experimental designs and study systems (Berlow *et al.* 2004).

Prediction 3: Warming decreases community stability at low and mild temperatures

Implications: If organisms currently experience temperatures below their optima (Pawar *et al.* 2016) and the functional response has a unimodal thermal dependence (Rall *et al.* 2012; Sentis *et al.* 2012; Uszko *et al.* 2017; Uiterwaal & DeLong 2020), consumer-resource interactions at low and mild temperatures will be destabilised by warming. At higher temperatures, however, warming should always enhance stability.

Reasoning: Stability in the context of consumer-resource interactions has predominantly referred to a 'qualitative' distinction between stable and oscillating dynamics (Rosenzweig & MacArthur 1963; Yodzis & Innes 1992; Vasseur & McCann 2005). We based our analysis on an adjusted version of a stability metric which quantifies the tendency of dynamics to oscillate (Johnson & Amarasekare 2015, SI 3). When comparing existing temperature parameterisations, we found that in most monotonic parameterisations, warming always (i.e., monotonically) stabilised dynamics (Fig. 7a, b, c). The single exception arose when warming and carrying capacity increased simultaneously, which in turn destabilised dynamics (Fig. 7f). Carrying capacity has been described as a proxy for enrichment and its destabilising effect has been established whether independently of temperature (Rosenzweig 1971) or as antagonistic to warming (Binzer *et al.* 2016). When at least one parameter in the functional response (i.e., attack rate or handling time) had a unimodal thermal dependence, this yielded a unimodal warming-stability relationship (Fig. 7d, e). Most significantly and perhaps surprisingly, the divergence between the unimodal and (most) monotonic parameterisations in the predicted effect of warming on stability manifested itself at low or mild, rather than high temperatures (Fig. 6, 7). This pattern originates in the impact of the parameters with unimodal thermal dependencies (i.e., attack rate and handling time) on stability. A hump-shaped thermal dependence of attack rate (Sentis *et al.* 2012; West & Post 2016; Uszko *et al.* 2017) produces a steep rise at low temperatures followed by a decreasing function at higher ones. Since attack

rate is destabilising (Table 1, McCann 2011), warming at low and mild temperatures – in a region of high sensitivity to attack rate (Fig. 7d) – will be strongly destabilising. However, further warming, where attack rate decreases, will be stabilising. Handling time, on the other hand, is stabilising close to the thermal extremes, (Fig. 6c, S5.2). Due to its U-shaped thermal dependence (Rall *et al.* 2012; West & Post 2016; Uszko *et al.* 2017) and the steepness of its slope at the extremes (SI 1), warming from low temperatures rapidly reduces handling time which is strongly destabilising; the reverse holds at high temperatures resulting in a strong stabilising effect. Thus, regardless of the thermal dependence shape of the functional response (attack rate and handling time), warming at high temperatures will be stabilising. However, at lower temperatures, unimodal and monotonic thermal dependencies produce contrasting warming-stability relationships. Therefore, the temperatures currently experienced by communities relative to their optimal temperature will determine the impact of warming on stability (Betini *et al.* 2019) in combination with the thermal dependence shape of the functional response.

Prediction 4: Warming stabilises dynamics only when interaction strength decreases faster than maximal energetic efficiency

Implications: The combination of ρ — the net energetic gain of consumers given unlimited resources — and κ — interaction strength — accurately describes the warming-stability relationship with no recourse to the thermal dependence shapes of individual parameters and assumptions about the current temperatures relative to the thermal optima or the proximity to the thermal boundaries of the community. Based on the Hopf bifurcation condition (eq. 11), a simple and unique relationship guarantees the stabilising effect of warming on consumer-resource interactions, namely that κ should decrease faster than ρ. Therefore, measuring ρ and

κ directly can increase the accuracy of warming-stability predictions and simplify cross-system comparisons.

Reasoning: Decreasing energetic efficiency or interaction strength have been used as an equivalent to increasing stability (Rall *et al.* 2008, 2010; Sentis *et al.* 2012). Thus, estimates of consumer energetic efficiency or interaction strength based on empirically-derived thermal dependence curves of individual rates (e.g. ingestion rate, attack rate, handling time, metabolic rate) have been used to infer the impacts of warming on stability (Rall *et al.* 2010, 2012; Vucic-Pestic *et al.* 2011; Sentis *et al.* 2012; Fussmann *et al.* 2014). However, this raises two significant issues. On the one hand, even subtle changes in the thermal dependence shapes of individual parameters can yield all possible outcomes (Amarasekare 2015). On the other hand, reducing the analysis of stability to a single aggregate parameter has limitations. Gilbert *et al.* (2014) described the warming-stability relationship with a single aggregate, interaction strength, but their approach was based on a type I functional response and its predictions do not work well in type II or III scenarios (Uszko *et al.* 2017). Johnson and Amarasekare (2015) and Amarasekare (2015), on the other hand, employed a simplifying assumption to attain a single aggregate parameter and reduce the complexity of their explorations. However, as the authors stated, this creates a 'conservative' stability metric and hence it lacks descriptive power of the dynamics close to the community's thermal boundaries (SI 3). Our analysis in the $\rho - \kappa$ plane suggests that stability cannot be reduced to a single aggregate parameter nor does a decrease in either one or both of ρ and κ suffice to stabilise dynamics. In fact, both ρ and κ can decrease with warming while dynamics become destabilised. As the Hopf bifurcation condition in the $\rho - \kappa$ plane reveals (Fig. 6a, dashed curve, eq. 11, $\kappa = \rho + 1$), a stabilising effect of warming requires not only a concurrent reduction in ρ and κ, but also the latter to decrease faster. Critically, both ρ and κ represent biological quantities which can be consistently

measured across study systems. Thus, directly measuring the thermal dependencies of ρ and κ would improve our understanding of the warming-stability relationship, while improving the accuracy of predictions by reducing the number of measurements and necessary assumptions.

Measuring the thermal dependence of the aggregate parameters

Our framework is based on two aggregate parameters, maximal consumer energetic efficiency, ρ, and interaction strength, κ. Maximal energetic efficiency measures the consumer maximal assimilated consumption as a fraction of its metabolic costs and therefore the net energetic gain of the consumer without resource limitation or consumer self-limitation (Yodzis & Innes 1992). Interaction strength is defined as the ratio of resource equilibrium density in the absence of consumers to the resource equilibrium density with consumers (Berlow *et al.* 1999; Gilbert *et al.* 2014). Past theoretical studies have proposed other pairs of aggregates including 'inverse resource abundance' or 'consumer thermal impact' (Yodzis & Innes 1992; Vasseur & McCann 2005). Though the choice of aggregate parameter pairs may be subject to fewer restrictions for theoretical applications, ρ and κ are well-suited for empirical approaches, as we argue below.

The fact that these aggregates constitute measurable quantities makes our framework a strong tool for bridging theoretical and empirical approaches. A targeted experiment to determine the thermal dependence of the maximal consumer energetic efficiency, ρ, can be to measure consumer population growth given unlimited resources. For interaction strength, κ, one can measure resource population density in presence and absence of consumers as often performed in field experiments where consumers are excluded (Berlow *et al.* 2004; Wootton & Emmerson 2005; Novak 2010; Estes *et al.* 2011). Measuring ρ and κ is thus relatively simple for consumer-resource pairwise interactions and can be done both in the laboratory and in the field.

In contrast, measuring the thermal dependencies of each single model parameter requires meticulous experiments that often can only be conducted in the laboratory in order to explore the entire temperature gradient. Our framework thus opens new avenues for investigating the effects of temperature on consumer-resource interactions using field experiments and data or by simplifying laboratory experiments. This should help multiply the numbers of biological systems with a characterised thermal dependence, allowing to test for generalities in the thermal dependence of consumer-resource interactions. Ultimately, working with ρ and κ will simplify experimental design by focusing on two quantifiable measures along the same temperature gradient used to build more classical temperature performance curves.

Framework subtleties

The sensitivity of both biomass ratio and stability to individual parameters varied depending on whether the consumer was close to the extinction boundary or far from it. Stability was most sensitive to changes in consumer assimilation efficiency and metabolism close to consumer extinction whereas changes in attack rate and carrying capacity were most important when far from consumer extinction (Fig. 6a). The importance of the functional response (attack rate) and the carrying capacity in determining the stability regime has been widely documented (Rosenzweig 1971; Amarasekare 2015; Johnson & Amarasekare 2015; Binzer *et al.* 2016; Uszko *et al.* 2017; Daugaard *et al.* 2019). Our results add the important caveat that this is the case only far from consumer extinction.

Regarding the sensitivity analysis, we should note that it quantified the intrinsic sensitivity of the model variables to local – infinitesimal – parameter changes. Therefore, applying its insights to data should take into consideration the scales of the individual parameters in the

temperature range of interest and rather importantly potential uncertainties in the parameter estimates (Manlik *et al.* 2018). That is why we argued for the reduced significance of assimilation efficiency in driving changes in biomass distributions, despite its high sensitivity.

Conclusions

Warming will have significant, but as yet uncertain impacts on consumer-resource interactions which underpin the structure and functioning of ecosystems. We presented a framework that will help to improve the accuracy of predictions and reconcile divergent results by facilitating cross-system comparisons. This framework first determines the parameters whose variations have the largest effect on community properties. Second, it simplifies analyses to a two-dimensional plane of mechanistically tractable aggregate parameters, maximal consumer energetic efficiency and interaction strength. Applying the framework to consumer-resource biomass ratio and stability, we showed that close to the consumer extinction boundary (i.e., at temperature extremes) both variables are most sensitive to changes in consumer assimilation efficiency and metabolism. Far from the boundary (i.e., mild temperatures), biomass ratio is most sensitive to resource growth rate, consumer assimilation efficiency and metabolism. This yielded our first prediction, that resource growth rate should regulate biomass distributions at mild temperatures. The consensus around the thermal dependence of metabolism and the limited potential impact of warming on assimilation efficiency, underscore the importance of correctly measuring the thermal dependence of resource growth rate. Using the two aggregate parameters not only added explanatory power to our analyses but simplified the study of important properties of consumer-resource interactions. From this followed our second prediction, that the thermal boundaries of the community are defined by interaction strength alone. In terms of stability, we demonstrated that a unimodal thermal dependence of attack rate

or handling time alters predictions with respect to the effects of warming on stability below the thermal optimum, where many organisms may be currently living. Hence our third prediction, that initial increases in mean temperatures will destabilise consumer-resource interactions. Significantly, our framework elucidates how the thermal dependence of stability can be comprehensively characterised by maximal energetic efficiency and interaction strength values, replacing measurements of multiple biological parameters. This produced our fourth prediction; a faster reduction of interaction strength than of maximal energetic efficiency with warming is necessary for dynamics to stabilise. Thus, targeted experiments to measure the thermal dependencies of maximal energetic efficiency and interaction strength would improve predictions. Ultimately, we show that any temperature parameterisation fitted to the Rosenzweig-MacArthur model can be mapped onto the aggregate parameter plane, revealing its stability landscape, providing a mechanistic interpretation for its predictions and allowing for the cross-system comparison of these predictions.

Acknowledgments

This research is supported by the FRAGCLIM Consolidator Grant, funded by the European Research Council under the European Union's Horizon 2020 research and innovation programme (Grant Agreement Number 726176).

References

Amarasekare, P. (2015). Effects of temperature on consumer-resource interactions. *J. Anim. Ecol.*, 84, 665–679.

Amarasekare, P. (2019). Effects of Climate Warming on Consumer-Resource Interactions: A

Latitudinal Perspective. *Front. Ecol. Evol.*, 7.

Archer, L.C., Sohlström, E.H., Gallo, B., Jochum, M., Woodward, G., Kordas, R.L., *et al.* (2019). Consistent temperature dependence of functional response parameters and their use in predicting population abundance. *J. Anim. Ecol.*, 88, 1670–1683.

Barbier, M. & Loreau, M. (2019). Pyramids and cascades: a synthesis of food chain functioning and stability. *Ecol. Lett.*, 22, 405–419.

Berlow, E.L., Navarrete, S.A., Briggs, C.J., Power, M.E. & Menge, B.A. (1999). Quantifying Variation in the Strengths of Species Interactions. *Ecology*, 80, 2206.

Berlow, E.L., Neutel, A.M., Cohen, J.E., De Ruiter, P.C., Ebenman, B., Emmerson, M., *et al.* (2004). Interaction strengths in food webs: Issues and opportunities. *J. Anim. Ecol.*

Betini, G.S., Avgar, T., McCann, K.S. & Fryxell, J.M. (2019). Temperature triggers a non-linear response in resource–consumer interaction strength. *Ecosphere*, 10.

Bideault, A., Galiana, N., Zelnik, Y.R., Gravel, D., Loreau, M., Barbier, M., *et al.* (2020). Thermal mismatches in biological rates determine trophic control and biomass distribution under warming. *Glob. Chang. Biol.*, gcb.15395.

Binzer, A., Guill, C., Brose, U. & Rall, B.C. (2012). The dynamics of food chains under climate change and nutrient enrichment. *Philos. Trans. R. Soc. B Biol. Sci.*, 367, 2935–2944.

Binzer, A., Guill, C., Rall, B.C. & Brose, U. (2016). Interactive effects of warming, eutrophication and size structure: impacts on biodiversity and food-web structure. *Glob. Chang. Biol.*, 22, 220–227.

Brown, J.H., Gillooly, J.F., Allen, A.P., Savage, V.M. & West, G.B. (2004). TOWARD A METABOLIC THEORY OF ECOLOGY. *Ecology*, 85, 1771–1789.

Caswell, H. (2019). *Sensitivity Analysis: Matrix Methods in Demography and Ecology*. Demographic Research Monographs. Springer International Publishing, Cham.

Dannon, E.A., Tamò, M., van Huis, A. & Dicke, M. (2010). Functional response and life

history parameters of Apanteles taragamae, a larval parasitoid of Maruca vitrata. *BioControl*, 55, 363–378.

Daugaard, U., Petchey, O.L. & Pennekamp, F. (2019). Warming can destabilize predator–prey interactions by shifting the functional response from Type III to Type II. *J. Anim. Ecol.*, 88, 1575–1586.

Dee, L.E., Okamtoto, D., Gårdmark, A. & Montoya, J.M. (2020). Temperature variability alters the stability and thresholds for collapse of interacting species. *BioRxiv*, 2020.05.18.102053.

Dell, A.I., Pawar, S. & Savage, V.M. (2011). Systematic variation in the temperature dependence of physiological and ecological traits. *Proc. Natl. Acad. Sci. U. S. A.*, 108, 10591–10596.

Deutsch, C.A., Tewksbury, J.J., Huey, R.B., Sheldon, K.S., Ghalambor, C.K., Haak, D.C., *et al.* (2008). Impacts of climate warming on terrestrial ectotherms across latitude. *Proc. Natl. Acad. Sci.*, 105, 6668–6672.

Easterling, D.R., Meehl, G.A., Parmesan, C., Changnon, S.A., Karl, T.R. & Mearns, L.O. (2000). Climate extremes: observations, modeling, and impacts. *Science*, 289, 2068–2074.

Ehnes, R.B., Rall, B.C. & Brose, U. (2011). Phylogenetic grouping, curvature and metabolic scaling in terrestrial invertebrates. *Ecol. Lett.*, 14, 993–1000.

Englund, G., Öhlund, G., Hein, C.L. & Diehl, S. (2011). Temperature dependence of the functional response. *Ecol. Lett.*, 14, 914–921.

Estes, J.A., Terborgh, J., Brashares, J.S., Power, M.E., Berger, J., Bond, W.J., *et al.* (2011). Trophic downgrading of planet earth. *Science (80-.).*

Fussmann, K.E., Schwarzmüller, F., Brose, U., Jousset, A. & Rall, B.C. (2014). Ecological stability in response to warming. *Nat. Clim. Chang.*, 4, 206–210.

Gilbert, B., Tunney, T.D., McCann, K.S., DeLong, J.P., Vasseur, D.A., Savage, V., *et al.*

(2014). A bioenergetic framework for the temperature dependence of trophic interactions. *Ecol. Lett.*, 17, 902–914.

Gilooly, J.F., Brown, J.H., Geoffrey, B.W., Savage, V.M. & Charnov, E.L. (2001). Effects of Size and Temperature on Metabolic Rate. *Science (80-.).*, 293, 2248–2251.

IPCC, 2013: *Climate Change 2013: The Physical Science Basis. Contribution of Working Group I to the Fifth Assessment Report of the Intergovernmental Panel on Climate Change* [Stocker, T.F., D. Qin, G.-K. Plattner, M. Tignor, S.K. Allen, J. Boschung, A. Nauels, Y. Xia, V. Bex and P.M. Midgley (eds.)]. Cambridge University Press, Cambridge, United Kingdom and New York, NY, USA, 1535 pp.

Jeschke, J.M., Kopp, M. & Tollrian, R. (2004). Consumer-food systems: Why type I functional responses are exclusive to filter feeders. *Biol. Rev. Camb. Philos. Soc.*

Johnson, C.A. & Amarasekare, P. (2015). A metric for quantifying the oscillatory tendency of consumer-resource interactions. *Am. Nat.*, 185, 87–99.

Lang, B., Ehnes, R.B., Brose, U. & Rall, B.C. (2017). Temperature and consumer type dependencies of energy flows in natural communities. *Oikos*, 126, 1717–1725.

Manlik, O., Lacy, R.C. & Sherwin, W.B. (2018). Applicability and limitations of sensitivity analyses for wildlife management. *J. Appl. Ecol.*, 55, 1430–1440.

May, R.M. (1972). Limit cycles in predator-prey communities. *Science (80-.).*, 177, 900–902.

McCann, K.S. (2011). *Food Webs (MPB-50) | Princeton University Press*. *Monograpsh Pop Bio*. Available at: https://press.princeton.edu/books/paperback/9780691134185/food-webs-mpb-50. Last accessed 10 September 2020.

Montoya, J.M. & Raffaelli, D. (2010). Climate change, biotic interactions and ecosystem services. *Philos. Trans. R. Soc. B Biol. Sci.*, 365, 2013–2018.

Novak, M. (2010). Estimating interaction strengths in nature: experimental support for an observational approach. *Ecology*, 91, 2394–2405.

O'Connor, M.I., Piehler, M.F., Leech, D.M., Anton, A. & Bruno, J.F. (2009). Warming and Resource Availability Shift Food Web Structure and Metabolism. *PLoS Biol.*, 7, e1000178.

Parmesan, C. (2006). Ecological and Evolutionary Responses to Recent Climate Change. *Annu. Rev. Ecol. Evol. Syst.*, 37, 637–669.

Pawar, S., Dell, A.I., Savage, V.M. & Knies, J.L. (2016). Real versus artificial variation in the thermal sensitivity of biological traits. *Am. Nat.*, 187, E41–E52.

Petchey, O.L., Brose, U. & Rall, B.C. (2010). Predicting the effects of temperature on food web connectance. *Philos. Trans. R. Soc. B Biol. Sci.*, 365, 2081–2091.

Pörtner, H.O. & Farrell, A.P. (2008). Ecology: Physiology and climate change. *Science (80-.).*

Rall, B., Guill, C. & Brose, U. (2008). Food-web connectance and predator interference dampen the paradox of enrichment. *Oikos*, 117, 202–213.

Rall, B.C., Brose, U., Hartvig, M., Kalinkat, G., Schwarzmüller, F., Vucic-Pestic, O., *et al.* (2012). Universal temperature and body-mass scaling of feeding rates. *Philos. Trans. R. Soc. B Biol. Sci.*, 367, 2923–2934.

Rall, B.Ö.C., Vucic-Pestic, O., Ehnes, R.B., EmmersoN, M. & Brose, U. (2010). Temperature, predator-prey interaction strength and population stability. *Glob. Chang. Biol.*, 16, 2145–2157.

Réveillon, T., Rota, T., Chauvet, É., Lecerf, A. & Sentis, A. (2019). Repeatable inter-individual variation in the thermal sensitivity of metabolic rate. *Oikos*, 128, 1633–1640.

Rip, J.M.K. & McCann, K.S. (2011). Cross-ecosystem differences in stability and the principle of energy flux. *Ecol. Lett.*, 14, 733–740.

Root, T.L., Price, J.T., Hall, K.R., Schneider, S.H., Rosenzweig, C. & Pounds, J.A. (2003). Fingerprints of global warming on wild animals and plants. *Nature*, 421, 57–60.

Rosenzweig, M.L. (1971). Paradox of Enrichment: Destabilization of Exploitation Ecosystems in Ecological Time. *Science (80-.).*, 171, 385–387.

Rosenzweig, M.L. & MacArthur, R.H. (1963). Graphical Representation and Stability Conditions of Predator-Prey Interactions. *Am. Nat.*, 97, 209–223.

Savage, V.M., Gilloly, J.F., Brown, J.H., Charnov, E.L. & Charnov, E.L. (2004). Effects of body size and temperature on population growth. *Am. Nat.*, 163, 429–41.

Sentis, A., Binzer, A. & Boukal, D.S. (2017). Temperature-size responses alter food chain persistence across environmental gradients. *Ecol. Lett.*, 20, 852–862.

Sentis, A., Hemptinne, J.L. & Brodeur, J. (2012). Using functional response modeling to investigate the effect of temperature on predator feeding rate and energetic efficiency. *Oecologia*, 169, 1117–1125.

Thakur, M.P., Künne, T., Griffin, J.N. & Eisenhauer, N. (2017). Warming magnifies predation and reduces prey coexistence in a model litter arthropod system. *Proc. R. Soc. B Biol. Sci.*, 284, 20162570.

Thomas, M.K., Kremer, C.T., Klausmeier, C.A. & Litchman, E. (2012). A global pattern of thermal adaptation in marine phytoplankton. *Science (80-.).*, 338, 1085–1088.

Uiterwaal, S.F. & DeLong, J.P. (2020). Functional responses are maximized at intermediate temperatures. *Ecology*.

Uszko, W., Diehl, S., Englund, G. & Amarasekare, P. (2017). Effects of warming on predator-prey interactions - a resource-based approach and a theoretical synthesis. *Ecol. Lett.*, 20, 513–523.

Vasseur, D.A. & McCann, K.S. (2005). A mechanistic approach for modeling temperature-dependent consumer-resource dynamics. *Am. Nat.*, 166, 184–98.

Vucic-Pestic, O., Ehnes, R.B., Rall, B.C. & Brose, U. (2011). Warming up the system: higher predator feeding rates but lower energetic efficiencies. *Glob. Chang. Biol.*, 17, 1301–

1310.

Walther, G.-R., Post, E., Convey, P., Menzel, A., Parmesan, C., Beebee, T.J.C., *et al.* (2002). Ecological responses to recent climate change. *Nature*, 416, 389–395.

West, D.C. & Post, D.M. (2016). Impacts of warming revealed by linking resource growth rates with consumer functional responses. *J. Anim. Ecol.*, 85, 671–680.

Wootton, J.T. & Emmerson, M. (2005). Measurement of Interaction Strength in Nature. *Annu. Rev. Ecol. Evol. Syst.*, 36, 419–444.

Yodzis, P. & Innes, S. (1992). Body size and consumer-resource dynamics. *Am. Nat.*, 139, 1151–1175.

Zhang, L., Takahashi, D., Hartvig, M. & Andersen, K.H. (2017). Food-web dynamics under climate change. *Proc. R. Soc. B Biol. Sci.*, 284, 20171772.

Zhao, Q., Liu, S. & Niu, X. (2020). Effect of water temperature on the dynamic behavior of phytoplankton–zooplankton model. *Appl. Math. Comput.*, 378, 125211.